

Projection-Free Evolution Strategies for Continuous Prompt Search

Yu Cai¹, Canxi Huang¹, and Xiaoyu He^{1,*}

Abstract—Continuous prompt search offers a computationally efficient alternative to conventional parameter tuning in natural language processing tasks. Nevertheless, its practical effectiveness can be significantly hindered by the black-box nature and the inherent high-dimensionality of the objective landscapes. Existing methods typically mitigate these challenges by restricting the search to a randomly projected low-dimensional subspace. However, the effectiveness and underlying motivation of the projection mechanism remain ambiguous. In this paper, we first empirically demonstrate that despite the prompt space possessing a low-dimensional structure, random projections fail to adequately capture this essential structure. Motivated by this finding, we propose a projection-free prompt search method based on evolutionary strategies. By directly optimizing in the full prompt space with an adaptation mechanism calibrated to the intrinsic dimension, our method achieves competitive search capabilities without additional computational overhead. Furthermore, to bridge the generalization gap in few-shot scenarios, we introduce a confidence-based regularization mechanism that systematically enhances the model’s confidence in the target verbalizers. Experimental results on seven natural language understanding tasks from the GLUE benchmark demonstrate that our proposed approach significantly outperforms existing baselines.

I. INTRODUCTION

Transformer-based pre-trained language models (PLMs) have gained significant attention in natural language processing applications such as text rephrasing and paraphrasing [1–3]. Recent studies have suggested that the performance of PLMs largely depends on the model size, and it is expected that, to approach human-level performance, a PLM must involve hundreds of billions of parameters [4]. However, tuning even a small number of parameters in this case could be prohibitively expensive, since a huge amount of activation memory is used in backpropagation. In addition, modern PLMs such as GPT-4 [5] are usually released as a service and directly updating their model parameters via traditional gradient methods is intractable.

Consequently, prompt search acts as an efficient alternative to parameter tuning methods. Prompt here refers to additional information, e.g., a common prefix sentence, which is fed into a PLM along with original input sentences. Prompt search treats PLMs as a black-box and optimizes some metrics over prompts rather than the model parameters. We focus on continuous prompt, where the prompt is a token sequence and the decision space of prompt search is

the product of individual embedding spaces of all involved tokens (or the “prompt space” for short).

The hardness of prompt search, in the sense of black-box optimization, lies in its high-dimensional nature. For example, RoBERTa-Large [6] has an embedding space of dimension 1,024, so searching for merely 50 prompt tokens leads to a problem of dimension 51,200. On the other hand, black-box optimization algorithms suffer from dimension-dependent slowdown in convergence rate, and thus may converge extremely slowly on high-dimensional landscapes [7]. Furthermore, modern black-box optimization algorithms, including both metaheuristics and those based on objective/gradient estimation, are seldom used when the problem has more than 10,000 dimensions due to the high computational cost [8]. Therefore, applying these methods directly to prompt search could be infeasible.

One representative work toward high-dimensional prompt search is the Black-Box Tuning (BBT) method proposed by Sun *et al.* [9]. BBT is a metaheuristic method based on projection. It assumes that high-quality prompts could be found in a low-dimensional affine subspace whose basis is fixed during the search. This admits running any black-box optimization algorithm in the reduced space, thereby addressing the aforementioned high-dimensional issue. Sun *et al.* suggested pre-defining the basis of the subspace via random sampling and then solving the space-reduced problem with Covariance Matrix Adaptation Evolution Strategy (CMA-ES) [10], a well-established metaheuristic based on second-order information approximation. Their method works well in several language understanding tasks and can even match the performance of standard full-parameter tuning methods [11].

Despite BBT’s success, the projection mechanism of BBT remains far from fully understood. For example, it assumes that the prompt space is intrinsically low-dimensional. Although this is partially supported by recent studies on the low-dimensional reparameterization of PLMs [12], it is unclear whether this holds in the prompt space. This raises our first research question.

Q1. Does the prompt space of PLMs really have a low-dimensional structure?

We answer this question affirmatively by showing that, on seven GLUE tasks, the prompt space has an intrinsic dimension of only a few hundred. In particular, we show empirically that there exists an upper bound on the estimated intrinsic dimension that does not increase consistently with the prompt length. This verifies the low-dimensional assumption adopted by BBT and similar work.

On the other hand, we note that the low intrinsic dimension nature of prompt search does not mean the existence of a

*Corresponding author: Xiaoyu He.

¹Y. Cai, C. Huang and X. He are with the School of Software Engineering, Sun Yat-sen University, Zhuhai, China (e-mail: caiy86@mail2.sysu.edu.cn; huangcx23@mail2.sysu.edu.cn; hexy73@mail.sysu.edu.cn).

global subspace that can capture high-quality prompts. In contrast, the low-dimensional projection of prompts is seen to be ineffective based on our experiments. We therefore propose to use projection-free alternatives to BBT to exploit the low intrinsic dimension. This leads to the second research question of this work.

Q2. How to efficiently perform prompt search without subspace projections?

We provide a straightforward yet effective approach based on the evolution strategy (ES) family of metaheuristics: instead of explicitly projecting prompts, we leave the decision space untouched and calibrate the adaptation mechanism to the intrinsic dimension, enabling standard ES variants to efficiently perform prompt search.

The final research question focuses on improving the generalization ability of our proposed projection-free methods:

Q3. How to regularize the objective of prompt search to promote generalization?

We identify that the overfitting risk in full-space search primarily stems from the model’s low global confidence in target verbalizers. Thereby, we introduce a confidence-based regularization term to the loss function, which significantly enhances the confidence in the involved verbalizers as well as the generalization performance.

This paper addresses the aforementioned questions by proposing a projection-free framework for continuous prompt search. Our method, while straightforward in design, yields performance that significantly surpasses existing baselines. The key findings are summarized below:

- We confirm the low-dimensional nature of the prompt search problem and quantify the intrinsic dimension.
- We show that standard ESs can efficiently perform prompt search in the full space by recalibrating the adaptation mechanism.
- We propose confidence-based regularization to enhance generalization for projection-free prompt search.

II. PRELIMINARIES

We formulate the prompt search problem and review BBT.

A. Problem Definition

Following [9], we formulate the continuous prompt of length l as a flattened vector $x \in \mathbb{R}^d$, where $d = l \cdot e$ represents the full prompt space dimension and e denotes the embedding size of the PLM \mathcal{M} .

The quality of a prompt $x \in \mathbb{R}^d$ is evaluated via querying \mathcal{M} on some data distribution conditioned on x . The task of prompt search can therefore be stated as:

$$\min_{x \in \mathbb{R}^d} f_{PS}(x) = \mathbb{E}_{(y,z) \sim \mathcal{D}} [\ell(\mathcal{M}(x \oplus y), z)] \quad (1)$$

where ℓ is a loss function, \mathcal{D} is a data distribution, (y, z) denotes a data sample containing an input sentence y and its corresponding label z , and \oplus denotes augmenting an input sentence with the prompt. The operation $x \oplus y$ transforms the input and prompt into the model’s embedding space through the following four steps: 1) preparing a template with specific placeholders; 2) placing the input y into the corresponding

placeholder locations; 3) computing the embedding vector of the resultant sentence; 4) concatenating the continuous prompt vector x with the embedding vector obtained.

We adapt \mathcal{M} for classification by evaluating log-likelihoods at the specific target position: the mask location for masked language models, or the first token following the prefix for causal language models. Let $\mathcal{M}(x \oplus y) \in \mathbb{R}^{|\mathcal{V}|}$ denote the logits over the vocabulary \mathcal{V} . The label z maps to a verbalizer subset $\mathcal{W} \subset \mathcal{V}$ (see Appendix II). We minimize the cross-entropy loss:

$$\ell_{CE}(\mathbf{a}, z) = - \sum_{v \in \mathcal{W}} \mathbb{I}\{v = z\} \log \left(\frac{\exp(a_v)}{\sum_{u \in \mathcal{W}} \exp(a_u)} \right) \quad (2)$$

where $a \in \mathbb{R}^{|\mathcal{V}|}$ represents the logits over the vocabulary and a_v corresponds to token v . Thus minimizing $\ell(\mathcal{M}(x \oplus y), z)$ increases the likelihood of producing the correct label z given an input y and the prompt x .

B. The BBT Method

BBT [9] is an evolutionary approach to solving problem (9). Its underlying algorithm is CMA-ES, a de facto standard metaheuristic for real-valued black-box optimization. CMA-ES explores the prompt space via sampling a multivariate Gaussian distribution, and the distribution is updated iteratively using landscape curvature information estimated via zeroth-order oracles. Hence it requires maintaining a covariance matrix of $d \times d$, leading to a quadratic complexity. BBT reduces the complexity by parameterizing prompts via a \tilde{d} -dimensional subspace and optimizing the following objective:

$$\min_{x \in \mathbb{R}^{\tilde{d}}} f_{\text{BBT}}(x; A, x_{\text{init}}) = f_{\text{PS}}(x_{\text{init}} + Ax) \quad (3)$$

where f_{PS} is given in (9). Here, $x_{\text{init}} \in \mathbb{R}^d$ and $A \in \mathbb{R}^{d \times \tilde{d}}$ denote the initial prompt (or anchor point) and the random projection matrix, respectively. Both terms are predefined and fixed throughout the search process. Hence, the decision space of (10) is a \tilde{d} -dimensional affine subspace with a fixed basis. With a sufficiently small \tilde{d} , the algorithmic overhead of CMA-ES can be made negligible.

III. LOW INTRINSIC DIMENSION OF PROMPT SPACE

As mentioned above, BBT randomly generates the initial prompt x_{init} and projection matrix A and fixes them during the search. This implicitly assumes 1) the existence of a global subspace in which the prompt search problem can be solved approximately, and 2) such a subspace can be constructed via random projections. We show in this section that these assumptions are not fully supported by empirical evidences. On one hand, we do find the prompt space admits a manifold which is of low dimension. On the other hand, random projection does not capture promising search regions, thereby not making problem-solving truly easier.

A. Low-Dimensional Manifold of Prompt Space

We investigate empirically the manifold geometry of the prompt space and show that it admits a low intrinsic dimension (ID). Our experiment involves a set of random prompts \mathcal{X} . Each prompt is uniformly sampled from the discrete prompt space \mathcal{V}^l and then cast into the continuous prompt space \mathbb{R}^d . To reflect the real hardness of prompt search, we explicitly evaluate the gradients of the objective (9) at these prompts as they capture the directions along which the prompts can be improved¹. Let $\mathcal{G} = \{\nabla f_{\text{PS}}(x)|x \in \mathcal{X}\}$ denote the gradient set, and we expect \mathcal{G} to form a low-dimensional manifold so prompts can be improved without exploring the full prompt space. We first normalize the gradients in \mathcal{G} to have zero mean and unit variance, and then compute their pairwise cosine distances. The intrinsic dimension of the manifold spanned by \mathcal{G} can now be estimated using the maximum likelihood estimation proposed in [13] as:

$$\hat{d} = \frac{1}{|\mathcal{X}|} \sum_{x \in \mathcal{X}} \left(\frac{1}{k-1} \sum_{j=1}^{k-1} \log \frac{T_k(x)}{T_j(x)} \right)^{-1},$$

where $T_k(x)$ denotes the distance of $\nabla f(x)$ to its k -th nearest neighbor in \mathcal{G} . This metric captures the minimum number of embedding dimensions needed for preserving the local neighborhood structure in \mathcal{G} .

General settings of the experiment are listed below. We set $|\mathcal{X}| = 5,000$. We use RoBERTa-Large as the backbone model [6]. We consider seven tasks from the GLUE benchmark [14], namely MRPC, MNLI, QQP, SST-2, RTE, CoLA, and QNLI. The experiment follows a 16-shot training setting. To ensure a thorough analysis, we evaluate the intrinsic dimension across a comprehensive range of prompt lengths l and neighborhood sizes k .

Fig. 1 plots the estimated intrinsic dimension \hat{d} across varying prompt lengths. The estimation proves robust to neighborhood size k and, crucially, does not increase proportionally with the prompt length. Instead, it consistently exhibits an empirical upper bound of approximately 250 across tasks. This confirms that the intrinsic dimension is orders of magnitude lower than the ambient dimension d , affirmatively answering Q1. This suggests prompt optimization is feasible within a low-dimensional manifold, independent of the full prompt space size. See Section V-C for sensitivity analysis.

B. The Limitations of Random Projections

Albeit in a low-dimensional manifold, prompts may not be easily improved in a subspace that is randomly generated and fixed during the search. To see this, we investigate two different approaches to performing prompt search: 1) solving the space-reduced problem (10) in $\mathbb{R}^{\hat{d}}$, and 2) solving original problem (9) directly in \mathbb{R}^d . We show that the first approach neither reduces the computation effort nor improves the solution quality compared with the second.

Let $x_* \in \mathbb{R}^d$ be the reference optimal prompt obtained in the full space for (9) and $y_* \in \mathbb{R}^{\hat{d}}$ the approximate solution

¹Gradient access is utilized solely for this analysis. All prompt search methods in this work operate under a gradient-free setting.

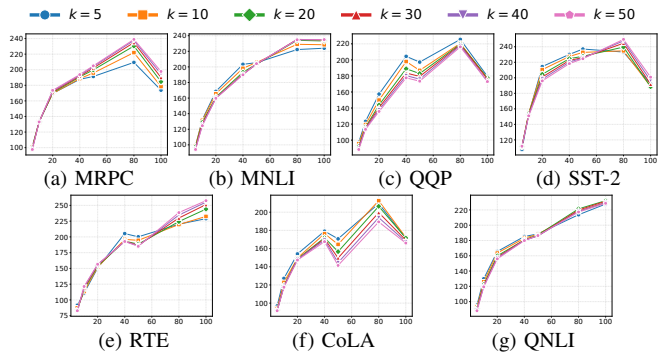


Fig. 1: Intrinsic dimension estimation on seven GLUE tasks. We report the estimated dimension (y-axis) across continuous prompt lengths $l \in \{5, 10, 20, 40, 50, 80, 100\}$ (x-axis). Different colors correspond to the neighborhood size $k \in \{5, 10, 20, 30, 40, 50\}$ used in the maximum likelihood estimation.

TABLE I: Comparison of training loss on the evaluated tasks. $f_{\text{PS}}(x_*)$ denotes the approximate optimal value in the full prompt space, while $f_{\text{BBT}}(y_*)$ corresponds to that in the random subspace.

	$f_{\text{PS}}(x_*)$	$f_{\text{BBT}}(y_*)$	γ_{OP}	γ_{PI}
MRPC	0.0250	0.0413	1.0072	1.4175
MNLI	0.2479	0.2738	0.9919	1.4001
QQP	0.0073	0.0310	0.9665	1.3856
SST-2	0.0051	0.0100	0.9590	1.3843
RTE	0.0611	0.0845	0.9632	1.3864
CoLA	0.0416	0.0698	0.9698	1.3878
QNLI	0.0156	0.0202	0.9886	1.4055

constrained in the subspace for (10). The solution y_* is obtained via running BBT in the reduced space, with an all-zero vector as the initial solution. To obtain x_* , we apply standard CMA-ES directly in the full prompt space to serve as a strong baseline. CMA-ES runs with the initial solution x_{init} , which is used in (10) for defining the subspace basis. This ensures the two formulations of prompt search, i.e., (9) and (10), are solved with the same initial prompts but in different spaces.

Apart from evaluating the objective values on x_* and y_* , we define the relative optimization progress, denoted by γ_{OP} , as a performance metric. It computes the ratio of the optimization progress made in solving (10) to that in solving (9):

$$\gamma_{\text{OP}} := \frac{\|(Ay_* + x_{\text{init}}) - x_{\text{init}}\|}{\|x_* - x_{\text{init}}\|},$$

where we measure the optimization progress of a method by the Euclidean distance of its obtained solution to the initial one. The lower the value of γ_{OP} is, the more efficient solving (10) is compared to solving (9).

Table VIII reports results on the same tasks as in Section III-A. We utilize a subspace dimension of $\hat{d} = 500$ (following BBT’s default) and a reduced prompt length of $l = 5$ to fit the computational constraints of full-space

CMA-ES (see Appendix III-C for detailed settings and a discussion on the fairness of this configuration). We find solving (9) always yields a lower training loss than solving (10), demonstrating superior prompts can be obtained by searching in the full space. Conversely, γ_{OP} is consistently close to 1 across all tasks. This implies that the subspace search does not effectively shorten the optimization trajectory. Instead, the projection primarily serves to circumvent the prohibitive computational costs of second-order methods in high dimensions, a challenge that can alternatively be addressed by employing simpler, scalable algorithms.

One may wonder if it is possible to trade the computation effort saved by solving (10) for a post-hoc improvement over the obtained solution. We show that it is also unlikely. To verify this, consider the following metric, which we call relative post-hoc improvement (denoted by γ_{PI}), defined as

$$\gamma_{PI} = \frac{\|x_* - (Ay_* + x_{init})\|}{\|x_* - x_{init}\|}.$$

The numerator quantifies the additional effort required to close the gap between the solution obtained for (10) and that for (9). A value of γ_{PI} greater than 1 means improving post-hocly the solution of (10) could be even more expensive than directly solving (9). Unfortunately, as reported in the last column of Table VIII, we do find γ_{PI} is above 1 in all considered tasks. This indicates that the random subspace projection limits the achievable solution quality, creating a performance gap not effectively bridged by merely extending the search budget.

IV. PROJECTION-FREE EVOLUTION STRATEGIES

Since random subspace projections offer limited efficiency gains while significantly hindering the search for optimal prompts, as shown in Section III-B, we propose a projection-free method to directly search within the full prompt space. We employ ES variants scaling linearly with the dimension, avoiding the quadratic complexity of covariance-based methods. However, these algorithms typically suffer from slow convergence in high-dimensional landscapes. To address this limitation and answer Q2, we introduce an ID-aware adaptation mechanism designed to accelerate optimization.

Algorithm 1 Standard (1+1)-ES and (1+1)-ES-ID

Require: objective function $f : \mathbb{R}^d \rightarrow \mathbb{R}$, initial step-size $\sigma^{[0]} \in \mathbb{R}_+$, initial solution $x^{[0]} \in \mathbb{R}^d$, intrinsic dimensions \tilde{d}

```

1: Setup damping factor:  $\tau = \sqrt{2d}$  or  $\tau = \sqrt{2\tilde{d}}$ 
2: for  $t = 0, 1, \dots$  do
3:    $u^{[t]} \sim \mathcal{N}(0, I_d)$  ▷ Mutation
4:    $s \leftarrow \mathbb{I}\{f(x^{[t]} + \sigma^{[t]}u^{[t]}) \leq f(x^{[t]})\}$  ▷ Success indicator
5:    $x^{[t+1]} = x^{[t]} + \sigma^{[t]}u^{[t]} \cdot s$  ▷ Descent
6:    $\sigma^{[t+1]} = \sigma^{[t]} \cdot \exp\left(\frac{1}{\tau}(s - \frac{1}{2})\right)$  ▷ Step-size adaptation
7: end for

```

A. ID-Aware Adaptation Mechanism

We employ two ES variants, the (1+1)-ES and the SaES (collectively referred to as standard ES in their original forms, and ES-ID when equipped with our adaptation), to

Algorithm 2 Standard SaES and SaES-ID

Require: objective function $f : \mathbb{R}^d \rightarrow \mathbb{R}$, initial step-size $\sigma^{[0]} \in \mathbb{R}_+$, initial solution $x^{[0]} \in \mathbb{R}^d$, population size λ , number of chosen solutions μ , intrinsic dimensions \tilde{d}

```

1: Setup damping factor:  $\tau = \sqrt{2d}$  or  $\tau = \sqrt{2\tilde{d}}$ 
2: for  $t = 0, 1, \dots$  do
3:   for  $i = 1, \dots, \lambda$  do
4:      $\delta_i^{[t]} \sim \mathcal{N}(0, 1)$  ▷ Step-size mutation
5:      $\sigma_i^{[t]} = \sigma^{[t]} e^{\delta_i^{[t]}/\tau}$  ▷ Trial step-size
6:      $u_i^{[t]} \sim \mathcal{N}(0, I_d)$  ▷ Solution mutation
7:      $x_i^{[t]} = x^{[t]} + \sigma_i^{[t]}u_i^{[t]}$  ▷ Trial solution
8:   end for
9:   Sort the solutions such that  $f(x_{1:\lambda}) \leq \dots \leq f(x_{\lambda:\lambda})$ 
10:   $x^{[t+1]} = \frac{1}{\mu} \sum_{i=1}^{\mu} x_{i:\lambda}^{[t]}$  ▷ Recombination
11:   $\sigma^{[t+1]} = \frac{1}{\mu} \sum_{i=1}^{\mu} \sigma_{i:\lambda}^{[t]}$  ▷ Step-size self-adaptation
12: end for

```

perform this projection-free search. Both methods operate via isotropic Gaussian mutation, parameterized by a mean vector $x^{[t]}$ and a global step-size $\sigma^{[t]}$. The (1+1)-ES is a single-individual elitist method that adjusts $\sigma^{[t]}$ based on the 1/5 success rule [15], while SaES utilizes a population-based self-adaptation mechanism where step-sizes are co-evolved. Detailed workflows are outlined in Algorithms 1 and 2.

Crucially, the step-size adaptation in both algorithms is governed by a damping factor τ . Standard theoretical guidelines recommend scaling τ with the ambient dimension ($\tau = \sqrt{2d}$). However, as verified in Section III-A, the prompt space admits a low-dimensional structure. Consequently, adhering to this conventional configuration results in excessively slow adaptation, where the step-size evolution is overly dampened by the high ambient dimensionality, hindering efficient convergence.

To address this, we propose the ID-aware adaptation mechanism that calibrates τ to the configured intrinsic dimension \tilde{d} rather than d . While $\tau = \sqrt{2d}$ is standard for general black-box optimization, our proposed $\tau = \sqrt{2\tilde{d}}$ provides a distinct hyperparameter recommendation tailored for tasks exhibiting such low-dimensional structure, like prompt search.

B. Numerical Studies

We first verify the training efficiency by comparing ES-ID against BBT and standard ES. For fair comparison, we configure the intrinsic dimension $\tilde{d} = 500$ for ES-ID to align with BBT's subspace dimensionality (see Section V-C for an in-depth analysis of this configuration). As illustrated in Section IV, SaES-ID achieves a training loss comparable to that of BBT within the limited budget of 5,000 function evaluations. This confirms that our ID-aware adaptation effectively enables direct full-space search to match the performance of subspace-based approaches on most tasks. In contrast, standard SaES often struggles to converge within this budget, as seen in CoLA. Although the single-individual (1+1)-ES-ID exhibits rapid initial descent, its aggressive adaptation combined with a lack of population diversity leads to premature convergence into local optima on tasks like MRPC.

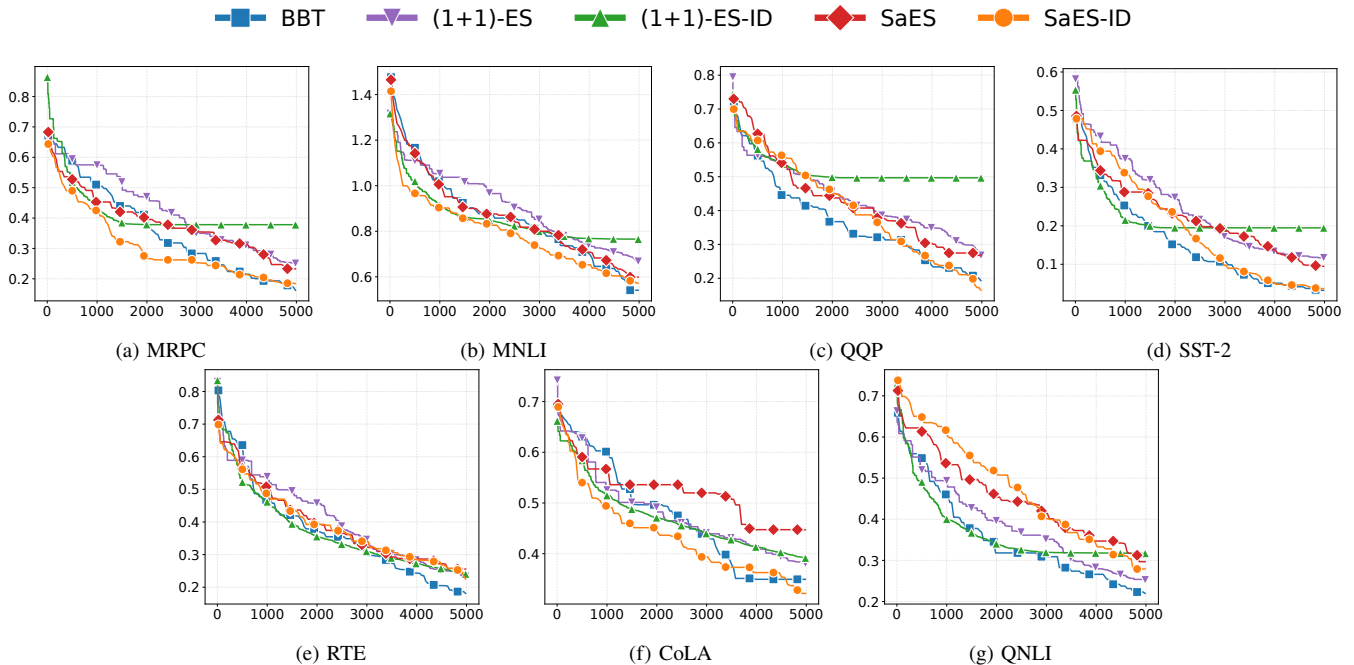


Fig. 2: Median performance on training data over 5 runs with different random seeds. Algorithms include (1+1)-ES, (1+1)-ES-ID, SaES, SaES-ID with projection-free and BBT with subspace projection. The x-axis denotes function evaluations, while the y-axis represents the loss function value.

Regarding generalization, however, Table II reveals that SaES-ID underperforms BBT on test metrics. While searching directly in the prompt space theoretically offers a higher performance upper bound, it is more susceptible to fitting noise in the few-shot setting. To address this, we propose a specialized regularization term in the next section. By explicitly modifying the optimization objective, this approach aims to mitigate such overfitting while simultaneously reshaping the landscape to facilitate (1+1)-ES-ID in escaping local optima.

V. CONFIDENCE-BASED REGULARIZATION

A. Motivation and Formulation

In standard continuous prompt search, model predictions are typically determined solely by the relative magnitudes of logits within the verbalizer set \mathcal{W} . Consequently, an optimized prompt might achieve a low cross-entropy loss by distinguishing between candidate verbalizers, yet the resulting prediction may still exhibit low confidence when evaluated against the entire vocabulary \mathcal{V} . We conjecture that this lack of global confidence is a primary driver of the observed poor generalization performance. Preliminary empirical analysis supports this hypothesis (see Appendix V), showing that unregularized methods indeed yield low-confidence predictions.

To bridge this gap, we introduce Confidence-based Regularization (CR). The regularized loss ℓ_{CR} is defined as:

$$\ell_{\text{CR}}(\mathbf{a}, z) = \ell_{\text{CE}}(\mathbf{a}, z) - \beta \cdot \log \left(\frac{\sum_{u \in \mathcal{W}} \exp(a_u)}{\sum_{v \in \mathcal{V}} \exp(a_v)} \right) \quad (4)$$

where ℓ_{CE} is the standard cross-entropy loss as defined in (9), and $\beta \in \mathbb{R}_+$ is a regularization coefficient. The newly

introduced term penalizes prompts yielding low confidence in candidate verbalizers, quantified by the ratio of summed logits between the verbalizer set and the vocabulary set.

Building upon this formulation, we incorporate ℓ_{CR} into our ES-ID method, yielding the variants (1+1)-ES-ID-CR and SaES-ID-CR (collectively ES-ID-CR). By minimizing ℓ_{CR} directly in the full prompt space, these algorithms enforce strictly high global confidence, leading to significantly improved generalization performance on downstream tasks.

B. Main Results

Table II presents the performance and average runtime of our projection-free methods compared to several baselines. Details of these baselines and experimental configurations are provided in Appendix I and Appendix III, respectively.

As illustrated, our proposed ES-ID-CR variants consistently outperform the baselines across the majority of tasks. In comparison to zero-shot baselines (ManualPrompt and ICL), ES-ID-CR demonstrates remarkably stable and superior performance, whereas zero-shot approaches exhibit high variance and suffer substantial performance drops on challenging datasets like CoLA. Furthermore, our approach achieves higher accuracy than few-shot optimization baselines such as BBT, BDPL, and ZOSGD. This superiority indicates that by searching directly in the full space coupled with confidence regularization, ES-ID-CR effectively mitigates the overfitting inherent in few-shot scenarios, yielding robust generalization.

Notably, internally, SaES-ID-CR achieves more substantial gains on MNLI and RTE compared to (1+1)-ES-ID-CR, benefiting from the robustness of population-based search.

TABLE II: Performance comparison on seven GLUE tasks. For our proposed projection-free methods with the CR term, results are reported using the optimal β . “Time/FE (s)” represents the average execution time per function evaluation. The results marked with \dagger are cited directly from [16]. Subscripts denote standard deviations.

Algorithm	MRPC F1	MNLI Acc	QQP F1	SST-2 Acc	RTE Acc	CoLA MCC	QNLI Acc	Time/FE s
ManualPrompt	77.69	40.80	29.37	78.10	50.18	0.79	48.70	-
ICL	48.13 _{12.0}	47.10 _{3.14}	45.73 _{7.01}	69.36 _{6.22}	54.15 _{2.79}	-0.54 _{2.67}	52.06 _{1.24}	-
BDPL \dagger	78.10 _{3.70}	42.50 _{1.80}	56.40 _{1.90}	87.60 _{2.10}	53.50 _{0.90}	4.60 _{1.20}	53.10 _{1.10}	-
RLPrompt \dagger	68.90 _{2.10}	42.80 _{3.20}	53.70 _{2.20}	88.40 _{1.90}	51.80 _{1.80}	5.00 _{1.10}	52.60 _{1.40}	-
BBT	77.33 _{0.00}	46.48 _{1.16}	51.09 _{2.38}	88.03 _{2.02}	54.30 _{1.66}	3.94 _{1.42}	54.30 _{1.23}	0.1442
ZOSGD	77.69 _{0.73}	46.42 _{1.28}	46.16 _{4.08}	86.74 _{0.41}	53.65 _{1.47}	-0.81 _{1.13}	59.00 _{1.42}	0.1498
ZOSGD-CR (ours)	79.37 _{1.60}	46.60 _{1.38}	54.04 _{1.11}	89.29 _{1.07}	54.66 _{2.59}	3.68 _{2.00}	59.48 _{1.85}	0.1499
(1+1)-ES	77.33 _{0.00}	46.42 _{1.28}	49.52 _{2.84}	86.95 _{0.71}	52.92 _{0.74}	4.67 _{2.13}	54.42 _{1.13}	0.1451
(1+1)-ES-ID (ours)	77.33 _{0.00}	46.42 _{1.28}	47.74 _{5.02}	86.95 _{2.06}	52.71 _{1.44}	3.71 _{1.15}	52.68 _{1.33}	0.1464
(1+1)-ES-ID-CR (ours)	81.50 _{0.10}	<u>49.04</u> _{1.43}	<u>54.37</u> _{0.84}	<u>89.66</u> _{0.98}	<u>56.10</u> _{1.16}	8.32 _{1.81}	<u>59.80</u> _{2.86}	0.1501
SaES	77.33 _{0.00}	46.54 _{1.05}	51.62 _{1.30}	87.41 _{1.38}	52.92 _{0.78}	5.20 _{2.60}	53.84 _{1.06}	0.1492
SaES-ID (ours)	77.33 _{0.00}	46.42 _{1.28}	50.93 _{3.51}	86.83 _{1.94}	53.86 _{1.70}	4.56 _{2.88}	52.88 _{0.89}	0.1503
SaES-ID-CR (ours)	<u>81.36</u> _{0.12}	52.44 _{1.09}	54.05 _{1.07}	90.37 _{1.20}	58.56 _{2.82}	4.75 _{1.73}	59.86 _{1.37}	0.1529

TABLE III: Sensitivity analysis of the CR coefficient β . We report the mean and standard deviation of performance over 5 runs.

Algorithm	MRPC	MNLI	QQP	SST-2	RTE	CoLA	QNLI
(1+1)-ES-ID-CR $\beta=0.01$	77.33 _{0.00}	46.42 _{1.28}	38.59 _{5.92}	86.88 _{1.48}	54.15 _{1.60}	-0.73 _{1.78}	59.80 _{2.86}
(1+1)-ES-ID-CR $\beta=0.1$	77.33 _{0.00}	46.50 _{1.22}	40.84 _{5.50}	88.65 _{1.49}	53.72 _{1.76}	0.74 _{2.29}	58.08 _{2.65}
(1+1)-ES-ID-CR $\beta=1$	77.76 _{0.64}	49.04 _{1.43}	53.32 _{1.39}	89.66 _{0.98}	56.10 _{1.16}	8.32 _{1.81}	53.24 _{2.46}
(1+1)-ES-ID-CR $\beta=10$	81.50 _{0.10}	48.72 _{1.18}	54.33 _{0.74}	79.50 _{2.05}	54.73 _{1.42}	6.16 _{1.79}	52.60 _{1.81}
(1+1)-ES-ID-CR $\beta=100$	79.71 _{1.95}	48.62 _{1.12}	54.37 _{0.84}	78.03 _{1.14}	53.79 _{0.65}	5.93 _{1.48}	51.00 _{1.72}
SaES-ID-CR $\beta=0.01$	77.33 _{0.00}	46.42 _{1.28}	48.52 _{3.96}	88.42 _{2.04}	54.22 _{1.92}	2.57 _{1.87}	59.86 _{1.37}
SaES-ID-CR $\beta=0.1$	77.33 _{0.00}	47.06 _{0.37}	52.83 _{1.17}	89.24 _{1.45}	54.15 _{1.43}	2.43 _{2.47}	59.36 _{1.32}
SaES-ID-CR $\beta=1$	78.58 _{1.19}	52.04 _{1.14}	54.05 _{1.07}	90.37 _{1.20}	58.56 _{2.82}	4.75 _{1.73}	52.76 _{1.84}
SaES-ID-CR $\beta=10$	81.36 _{0.12}	51.52 _{1.10}	51.55 _{5.51}	82.64 _{5.38}	54.01 _{0.49}	4.63 _{3.53}	51.04 _{1.32}
SaES-ID-CR $\beta=100$	81.20 _{0.26}	52.44 _{1.09}	50.54 _{7.54}	77.80 _{0.80}	53.79 _{0.51}	3.15 _{1.63}	50.52 _{1.34}

Further analysis demonstrates that ES-ID-CR significantly outperforms both standard ESs and ES-ID variants. Specifically, the ID-aware adaptation enables efficient convergence within the full prompt space, while CR serves as a critical regularizer to enhance generalization. To evaluate the universality of this regularization, we extend our method to ZOSGD. Results show that ZOSGD-CR achieves substantial improvement over standard ZOSGD, confirming CR as an effective, plug-and-play module applicable to other gradient-free optimizers. However, ZOSGD-CR still underperforms compared to ES-ID-CR. This gap arises because ZOSGD relies on pre-defined learning rate schedules rather than dimension-dependent adaptive mechanisms, fundamentally limiting its ability to exploit the intrinsic dimension for accelerated convergence.

Finally, regarding computational efficiency, the ‘Time/FE’ results show that our projection-free methods incur negligible overhead compared to BBT, maintaining competitive training speed despite searching in the full prompt space.

C. Sensitivity Analysis

To further understand our methods, we analyze the sensitivity of two key hyperparameters: the intrinsic dimension \tilde{d} and the regularization coefficient β .

a) *Robustness to Intrinsic Dimension \tilde{d} .*: To assess the sensitivity of the configured intrinsic dimension, we evaluate ES-ID-CR using fixed β across a discrete set of values $\tilde{d} \in \{50, 100, 200, 300, 500, 1000\}$. As illustrated in Fig. 3, the test performance stabilizes once \tilde{d} exceeds the empirical upper bound (≈ 250) identified in Section III-A, maintaining robust results across the sufficient dimension regime.

Consequently, we set $\tilde{d} = 500$ for our main experiments². This selection serves a dual purpose: it acts as a heuristic safety margin that comfortably exceeds the identified empirical bound to ensure manifold coverage, and simultaneously ensures fairness in comparison by aligning with the subspace dimensionality of the BBT baseline.

b) *Impact of Regularization Coefficient β .*: With \tilde{d} fixed at 500, we investigate the regularization coefficient β across a geometric progression $\{0.01, 0.1, 1, 10, 100\}$. Mathematically, β serves as a weighting coefficient that governs the trade-off between the standard cross-entropy loss and the CR term. Specifically, a value of $\beta < 1$ prioritizes the cross-entropy loss, focusing the optimization on minimizing

²The exploratory analysis in Section III-A confirms that the intrinsic dimension consistently exhibits an upper bound of magnitude 10^2 . This general physical property justifies treating \tilde{d} as a fixed, tuning-free hyperparameter, eliminating the need for task-specific gradient measurements during the black-box search phase.

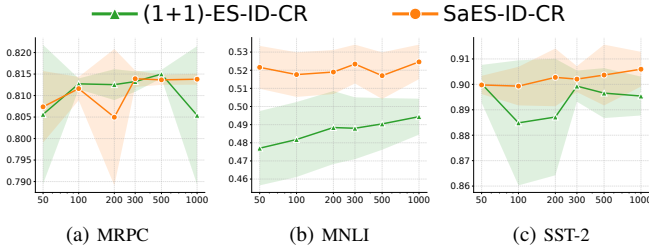


Fig. 3: Sensitivity analysis of intrinsic dimension \tilde{d} . We report the mean and standard deviation of performance over 5 runs.

TABLE IV: Performance comparison on GLUE tasks using the causal OPT-6.7B model.

Task	BBT	(1+1)-ES-ID-CR	SaES-ID-CR
MRPC	57.33 _{8.04}	74.00 _{9.47}	80.18 _{2.26}
MNLI	32.92 _{1.33}	30.70 _{1.16}	33.54 _{2.40}
QQP	50.41 _{3.28}	48.02 _{6.55}	54.77 _{3.22}
SST-2	81.22 _{3.15}	71.88 _{3.86}	86.17 _{1.84}
RTE	56.53 _{1.75}	54.95 _{2.78}	57.76 _{1.66}
CoLA	10.30 _{0.94}	11.42 _{4.43}	8.40 _{0.60}
QNLI	58.22 _{1.58}	56.30 _{0.94}	58.46 _{0.35}

prediction error, whereas $\beta > 1$ shifts the focus toward enforcing strictly high-confidence predictions.

As shown in Table III, the parameter sensitivity exhibits a remarkably consistent pattern. For any given task, the values yielding near-optimal performance tend to congregate within a specific magnitude regime rather than appearing as discrete, scattered peaks. This smooth sensitivity landscape implies that determining β does not necessitate computationally expensive fine-grained tuning. Instead, a coarse-grained search is sufficient to identify the effective regime, identifying whether a task requires dominance by cross-entropy ($\beta < 1$), a balanced objective ($\beta \approx 1$), or strong regularization ($\beta > 1$).

D. Generality across Model Architectures

To verify generality beyond masked LMs, we evaluate our method on the causal LM OPT-6.7B [17]. Despite the challenges of large-scale causal models (e.g., expanded parameter space), SaES-ID-CR significantly outperforms BBT on 6/7 tasks (Table IV), notably boosting MRPC from 57.33 to 80.18 and SST-2 from 81.22 to 86.17. Conversely, (1+1)-ES-ID-CR is less consistent, highlighting that SaES’s population diversity is essential for stable optimization in larger search spaces. These results confirm our method’s cross-architecture effectiveness.

VI. RELATED WORK

A. Intrinsic Dimensions of PLMs

The intrinsic dimension refers to a measurable property within metric spaces that significantly impacts search efficiency [18]. Recent studies have measured the intrinsic dimension in the parameter space of neural networks [19].

Notably, the intrinsic dimension of the PLM parameter space can be substantially lower than its ambient dimensionality when applied to common NLP tasks [12]. Existing research on prompt search assumes a low intrinsic dimension in the prompt space and adopts the same subspace projection technique previously applied to the parameter space to exploit this property [9, 11]. However, formal verification of whether this intrinsic dimension hypothesis holds in the prompt space is still lacking.

B. Black-Box Prompt Search

Prompt search is inherently black-box as PLMs expose only input-output behavior. While Evolution Strategies are well-suited for this setting, complex variants like CMA-ES are computationally prohibitive in high-dimensional prompt spaces. Consequently, recent works often rely on subspace projection to make optimization feasible [20]. Beyond ES, Zeroth-Order SGD [21] offers an efficient gradient-free alternative for continuous prompts. In the discrete setting, Reinforcement Learning approaches [16, 22] shows strong performance treating prompt tokens as actions or weak classifiers.

VII. CONCLUSION

In this work, we propose a projection-free method for black-box prompt search. We measure the intrinsic dimension of the prompt space, observing it exhibits an empirical upper bound independent of prompt length. Guided by this, we design an ID-aware adaptation mechanism enabling efficient search in the full prompt space, bypassing the misalignment of random projections. To address the generalization gap, we incorporate confidence-based regularization enforcing high global confidence. Extensive experiments demonstrate that our approach significantly outperforms baselines across GLUE tasks and generalizes robustly to large-scale causal architectures.

APPENDIX I BASELINES

To evaluate the effectiveness of our approach, we compare our proposed methods against several distinct categories of baselines evaluated on the RoBERTa-Large model:

- **ManualPrompt**: A zero-shot baseline that utilizes the handcrafted templates listed in Table V to evaluate performance without training.
- **In-Context Learning (ICL)**: Evaluates the model’s few-shot capability by prefixing the input with labeled examples [23]. The number of demonstration examples equals the number of label categories, where one example is randomly selected from the training set corresponding to each specific label.
- **BBT** [9]: A continuous prompt search method that employs CMA-ES to optimize prompts within a projected subspace.
- **RLPrompt** [22]: A discrete prompt search framework that formulates prompt generation as a standard reinforcement learning task, training an agent to generate high-quality token sequences.

- **BDPL** [16]: A discrete prompt optimization approach that employs a variance-reduced policy gradient strategy to optimize discrete prompt tokens in a gradient-free manner.
- **ZOSGD** [24]: A gradient-free optimizer that approximates gradients using finite differences. In our experiments, it is applied directly to the full prompt space under the same 16-shot setting to serve as a high-dimensional optimization baseline.

A. Additional Baseline Experimental Results

In this section, we provide supplementary experimental results for the ZOSGD-CR, BDPL, and RLPrompt baselines as presented in Table VII.

a) ZOSGD-CR Sensitivity Analysis: In the main text, we reported the performance of ZOSGD-CR using the optimal hyperparameter configuration. Here, we investigate the impact of the regularization strength. We fixed the base learning rate at $1e-2$ and the sampling radius at $1e-4$, while presenting the complete results across varying regularization coefficients $\beta \in \{0.01, 0.1, 1, 10, 100\}$. As evidenced in Table VII, the method exhibits a consistent preference for $\beta \approx 1$ across most tasks.

TABLE V: Templates and label descriptions for the mask-filling RoBERTa-Large model.

Dataset	Template	Verbalizers
MRPC	$s_1?$ [MASK], s_2 .	yes / no
MNLI	$s_1?$ [MASK], s_2 .	yes / maybe / no
QQP	s_1 [MASK], s_2 .	yes / no
SST-2	s_1 . It was [MASK].	great / terrible
RTE	$s_1?$ [MASK], s_2 .	yes / no
CoLA	s_1 Correct? [MASK].	yes / no
QNLI	$s_1?$ [MASK], s_2 .	yes / no

TABLE VI: TEMPLATES AND LABEL DESCRIPTIONS FOR THE CAUSAL OPT-6.7B MODEL

Dataset	Template	Verbalizers
MRPC	input: sentence one: s_1 sentence two: s_2 equivalent? \n output:	yes / no
MNLI	input: sentence one: s_1 sentence two: s_2 entailment? \n output:	yes / maybe / no
QQP	input: sentence one: s_1 sentence two: s_2 equivalent? \n output:	yes / no
SST-2	input: s_1 It was \n output:	great / terrible
RTE	input: sentence one: s_1 sentence two: s_2 entailment? \n output:	yes / no
CoLA	input: s_1 correct? \n output:	yes / no
QNLI	input: sentence one: s_1 sentence two: s_2 entailment? \n output:	yes / no

b) Baseline Reproduction and Analysis: To ensure a rigorous comparative study, we reproduced the discrete optimization baselines, BDPL [16] and RLPrompt [22], strictly adhering to the hyperparameter configurations and computational budgets recommended in their original literature.

We observe that the reproduction results under our unified 16-shot protocol are generally lower than the best results reported in the original papers. We attribute this to two technical factors inherent to the unified evaluation setting:

- **Metric-Reward Misalignment in RLPrompt:** The default reward function in the official RLPrompt implementation is designed to optimize prediction accuracy. This creates an objective mismatch for tasks evaluated on disjoint metrics such as F1 score (MRPC, QQP) or MCC (CoLA). Without task-specific reward engineering (which introduces additional manual intervention), the policy learning remains suboptimal for these specific metrics.
- **Sensitivity in Discrete Search:** Methods like BDPL are known to be sensitive to seed variations in few-shot scenarios. Our reproduction reflects the average performance under a standard, unrefined execution without extensive random seed searching.

Note on Fairness: We observed that the BDPL literature [16] reported significantly higher performance for RLPrompt compared to our local reproduction, although the specific implementation details yielding these results were not fully disclosed. Given the high overlap between our evaluation tasks and those in [16], we adopt the most rigorous comparison strategy: in the main text (Table 2), we cite the reported results from [16] for both their proposed method (BDPL) and the RLPrompt baseline. The local reproduction results in Table VII are provided solely to illustrate the methods’ behavior under a constrained, out-of-the-box experimental setting.

APPENDIX II BACKBONE MODELS AND TEMPLATES

We conduct experiments on two distinct pre-trained language models to verify the generality of our framework: RoBERTa-Large (355M parameters), representative of masked language models, and OPT-6.7B (6.7B parameters), representative of large-scale causal language models.

For each task, we assign specific manual templates and verbalizers. We primarily adopt the templates from BDPL [16] with minor modifications to fit the respective model architectures. Table V and Table VI provide the detailed configurations for RoBERTa-Large and OPT-6.7B, respectively.

APPENDIX III EXPERIMENTAL SETTINGS

All experiments are carried out on NVIDIA RTX 4090 GPUs. We adhere to the standard few-shot experimental setting, where $K = 16$ samples are randomly selected per class to construct the training and validation sets, respectively, with model selection determined by validation performance.

Regarding evaluation metrics, we follow the protocols established in prior studies [16] Specifically, we adopt the Matthews Correlation Coefficient (MCC) for CoLA, and the F1-score for MRPC and QQP. For other tasks, including SST-2, RTE, and QNLI, we utilize accuracy as the performance metric. Distinct from the average strategy, we explicitly

TABLE VII: Additional experimental results for ZOSGD-CR, BDPL, and RLPrompt. We report the mean and standard deviation over 5 independent runs.

Algorithm	MRPC	MNLI	QQP	SST-2	RTE	CoLA	QNLI
ZOSGD-CR $\beta=0.01$	77.33 _{0.00}	46.42 _{1.28}	44.74 _{4.27}	86.63 _{0.40}	53.65 _{1.24}	-0.25 _{1.48}	58.58 _{1.90}
ZOSGD-CR $\beta=0.1$	77.58 _{0.51}	46.54 _{1.09}	48.47 _{2.54}	87.68 _{0.52}	54.66 _{2.59}	1.49 _{2.41}	59.48 _{1.85}
ZOSGD-CR $\beta=1$	79.37 _{1.60}	46.42 _{1.28}	54.04 _{1.11}	89.29 _{1.07}	54.30 _{0.54}	3.68 _{2.00}	51.66 _{1.01}
ZOSGD-CR $\beta=10$	77.95 _{1.23}	46.60 _{1.38}	48.63 _{7.77}	84.61 _{2.17}	53.86 _{0.27}	1.91 _{1.64}	50.46 _{1.38}
ZOSGD-CR $\beta=100$	77.46 _{0.27}	46.42 _{1.28}	48.23 _{8.85}	82.39 _{4.15}	53.57 _{0.43}	3.45 _{3.85}	51.18 _{1.76}
BDPL (Ours)	68.63 _{4.95}	25.76 _{1.97}	52.40 _{1.21}	83.85 _{1.57}	52.78 _{2.38}	1.95 _{4.20}	54.35 _{1.40}
RLPrompt (Ours)	47.53 _{1.18}	48.73 _{2.23}	49.11 _{2.00}	84.58 _{3.12}	56.61 _{2.27}	-1.66 _{2.63}	51.19 _{1.20}

report the accuracy on the matched validation set for MNLI. All reported results are averaged over 5 independent runs using seeds $\{0, 1, 42, 43, 100\}$.

Regarding the optimization configuration, unless otherwise stated, all algorithms operate with a budget of 5,000 function evaluations (FEs). To align the search dimensionality across different model scales, we configure the continuous prompt length as $l = 50$ for RoBERTa-Large and $l = 10$ for OPT-6.7B.

A. Settings for Intrinsic Dimension Analysis

For the intrinsic dimension analysis in Section II, we employ Maximum Likelihood Estimation (MLE) on the gradient manifold. The estimation is performed using a sample size of $|\mathcal{X}| = 5,000$ to ensure statistical stability. We vary the continuous prompt length $l \in \{5, 10, 20, 40, 50, 80, 100\}$ to verify the scaling behavior. Note that gradient access via backpropagation is utilized *solely* for this specific geometric analysis, while the proposed prompt search methods remain strictly gradient-free.

B. Settings for Subspace Necessity Analysis

In Appendix IV, we investigate the necessity of random subspace projections by comparing subspace-based optimization against direct full-space optimization. To ensure a rigorous conclusion, this comparative study adopts a specific configuration distinct from the main experiments.

a) Optimization Algorithm.: To eliminate algorithmic variables as confounding factors, we employ the exact same optimizer, standard CMA-ES, for both the subspace and full-space settings. Note that while CMA-ES serves as a rigorous baseline for this theoretical analysis, its quadratic complexity makes it intractable for the high-dimensional main experiments, necessitating the scalable evolutionary strategies (e.g., SaES) used there.

b) Prompt Length and Dimensionality.: Standard CMA-ES incurs a space complexity of $O(d^2)$. For the default prompt length of $l = 50$ ($d = 51,200$), maintaining the covariance matrix would require storing over 2.6 billion parameters, which is computationally prohibitive. Consequently, we reduce the prompt length to $l = 5$ ($d = 5,120$) exclusively for this analysis. This reduction makes full-space covariance adaptation feasible while preserving the problem’s fundamental geometric characteristics.

c) Computational Budget.: Black-box optimization algorithms inherently suffer from dimension-dependent convergence slowdowns. To accommodate the increased difficulty of searching in the full parameter space ($d = 5,120$) compared to the subspace ($\tilde{d} = 500$), we extend the budget to 10,000 function evaluations (FEs), ensuring sufficient convergence opportunity for the full-space baseline.

d) Fairness of the Configuration.: We emphasize that this setup ($l = 5, \tilde{d} = 500$) is theoretically *biased towards* the subspace approach. The random subspace covers $\approx 10\%$ of the degrees of freedom, a significantly higher proportion than in the standard setting ($< 1\%$). If random projections fail to demonstrate effectiveness in this relaxed setting, their utility in the stricter, high-dimensional standard setting is even less probable.

C. Step-Size Alignment for Fair Comparison

In the comparative experiments detailed in Section III, we utilize RoBERTa-Large with a prompt length of $l = 50$ and an embedding dimension of $e = 1,024$, resulting in a full prompt space dimension of $d = 51,200$. The subspace dimension for BBT is set to $\tilde{d} = 500$.

Regarding the hyperparameter configuration, we apply a consistent alignment strategy across all algorithms, including the BBT baseline and our projection-free variants (standard ES and ES-ID). Specifically, we set the initial step-size $\sigma^{[0]} = 1$ for BBT and $\sigma^{[0]} = 1/\sqrt{3}$ for all ES variants. The value of 1 for BBT follows the default setting in the original paper [9]. The value of $1/\sqrt{3}$ for the ES variants is analytically derived to ensure that the variance of the update vectors in the full prompt space aligns with that of BBT, thereby guaranteeing a fair comparison of exploration efficiency.

This differentiation is necessary because the methods operate in different spaces. While BBT performs optimization in a low-dimensional subspace, its updates are projected into the full parameter space \mathbb{R}^d via a random matrix \mathbf{A} . This projection implicitly scales the magnitude of the update vectors. To ensure that our projection-free methods operating directly in \mathbb{R}^d maintain an identical initial exploration granularity (i.e., expected update energy), we align the variances of their update vectors as follows.

Let Δ_{ES} and Δ_{BBT} denote the update vectors in the full space for ES and BBT, respectively. For ES, the update is given by $\Delta_{\text{ES}} = \sigma_{\text{ES}} \cdot \mathbf{u}$, where $\mathbf{u} \sim \mathcal{N}(\mathbf{0}, \mathbf{I}_d)$. The expected

squared Euclidean norm is:

$$\mathbb{E}[\|\Delta_{\text{ES}}\|^2] = \sigma_{\text{ES}}^2 \cdot \mathbb{E}[\|\mathbf{u}\|^2] = \sigma_{\text{ES}}^2 \cdot d. \quad (5)$$

For BBT, the update is $\Delta_{\text{BBT}} = \mathbf{A}(\sigma_{\text{BBT}} \cdot \mathbf{z})$, where $\mathbf{z} \sim \mathcal{N}(\mathbf{0}, \mathbf{I}_{\tilde{d}})$ and entries of \mathbf{A} are sampled from $U[-\frac{1}{\sqrt{\tilde{d}}}, \frac{1}{\sqrt{\tilde{d}}}]$.

The expected squared norm is calculated as:

$$\begin{aligned} \mathbb{E}[\|\Delta_{\text{BBT}}\|^2] &= \sigma_{\text{BBT}}^2 \mathbb{E}_{\mathbf{A}, \mathbf{z}}[\text{Tr}(\mathbf{z}^\top \mathbf{A}^\top \mathbf{A} \mathbf{z})] \\ &= \sigma_{\text{BBT}}^2 \mathbb{E}_{\mathbf{A}}[\text{Tr}(\mathbf{A} \mathbf{A}^\top)] \\ &= \sigma_{\text{BBT}}^2 \sum_{i=1}^d \sum_{j=1}^{\tilde{d}} \mathbb{E}[A_{i,j}^2]. \end{aligned} \quad (6)$$

Given that $\mathbb{E}[A_{i,j}^2] = \frac{1}{3\tilde{d}}$ for the uniform distribution, we obtain:

$$\mathbb{E}[\|\Delta_{\text{BBT}}\|^2] = \sigma_{\text{BBT}}^2 \cdot (d \cdot \tilde{d}) \cdot \frac{1}{3\tilde{d}} = \sigma_{\text{BBT}}^2 \cdot \frac{d}{3}. \quad (7)$$

By equating Equations (1) and (3) to match the update energy ($\mathbb{E}[\|\Delta_{\text{ES}}\|^2] = \mathbb{E}[\|\Delta_{\text{BBT}}\|^2]$), we find that $\sigma_{\text{ES}}^2 \cdot d = \sigma_{\text{BBT}}^2 \cdot \frac{d}{3}$, which simplifies to:

$$\sigma_{\text{ES}} = \frac{\sigma_{\text{BBT}}}{\sqrt{3}}. \quad (8)$$

Consequently, with the baseline setting $\sigma_{\text{BBT}} = 1$, we configure $\sigma^{[0]} = 1/\sqrt{3}$ for the ES variants (standard ES and ES-ID) in our comparative experiments.

D. Hyperparameters for Main Results

In the main experiments, we evaluate the ES-ID-CR variants. The introduction of the confidence regularization (CR) term significantly reshapes the objective landscape, necessitating a recalibration of the initial step size $\sigma^{[0]}$ rather than adhering to the theoretical value derived in Appendix III-C. Consequently, we performed a grid search for the initial step size within $\sigma^{[0]} \in \{1, 10^{-1}, 10^{-2}, 10^{-3}, 10^{-4}\}$ and for the regularization coefficient within $\beta \in \{100, 10, 1, 0.1, 0.01\}$.

For RoBERTa-Large ($l = 50$), based on the search results, we configure $\sigma^{[0]} = 10^{-4}$ for (1+1)-ES-ID-CR and $\sigma^{[0]} = 10^{-2}$ for SaES-ID-CR.

For OPT-6.7B, we adjusted the prompt length to $l = 10$. This setting is adopted because prompt tuning becomes less sensitive to prompt length as model scale increases [25], and it aligns the computational burden with the RoBERTa-Large experiments under the same query budget. For this model, we set $\sigma^{[0]} = 1$ for both (1+1)-ES-ID-CR and SaES-ID-CR.

APPENDIX IV

THE LIMITATIONS OF RANDOM PROJECTIONS

$$\min_{x \in \mathbb{R}^d} f_{\text{PS}}(x) = \mathbb{E}_{(y,z) \sim \mathcal{D}}[\ell(\mathcal{M}(x \oplus y), z)] \quad (9)$$

$$\min_{x \in \mathbb{R}^{\tilde{d}}} f_{\text{BBT}}(x; A, x_{\text{init}}) = f_{\text{PS}}(x_{\text{init}} + Ax) \quad (10)$$

Albeit in a low-dimensional manifold, prompts may not be easily improved in a subspace that is randomly generated and fixed during the search. To see this, we investigate two different approaches to performing prompt search: 1)

TABLE VIII: Comparison of training loss on the evaluated tasks. $f_{\text{PS}}(x_*)$ denotes the approximate optimal value in the full prompt space, while $f_{\text{BBT}}(y_*)$ corresponds to that in the random subspace.

	$f_{\text{PS}}(x_*)$	$f_{\text{BBT}}(y_*)$	γ_{OP}	γ_{PI}
MRPC	0.0250	0.0413	1.0072	1.4175
MNLI	0.2479	0.2738	0.9919	1.4001
QQP	0.0073	0.0310	0.9665	1.3856
SST-2	0.0051	0.0100	0.9590	1.3843
RTE	0.0611	0.0845	0.9632	1.3864
CoLA	0.0416	0.0698	0.9698	1.3878
QNLI	0.0156	0.0202	0.9886	1.4055

solving the space-reduced problem (10) in $\mathbb{R}^{\tilde{d}}$, and 2) solving original problem (9) directly in \mathbb{R}^d . We show that the first approach neither reduces the computation effort nor improves the solution quality compared with the second.

Let $x_* \in \mathbb{R}^d$ be the reference optimal prompt obtained in the full space for (9) and $y_* \in \mathbb{R}^{\tilde{d}}$ the approximate solution constrained in the subspace for (10). The solution y_* is obtained via running BBT in the reduced space, with an all-zero vector as the initial solution. To obtain x_* , we apply standard CMA-ES directly in the full prompt space to serve as a strong baseline. CMA-ES runs with the initial solution x_{init} , which is used in (10) for defining the subspace basis. This ensures the two formulations of prompt search, i.e., (9) and (10), are solved with the same initial prompts but in different spaces.

Apart from evaluating the objective values on x_* and y_* , we define the relative optimization progress, denoted by γ_{OP} , as a performance metric. It computes the ratio of the optimization progress made in solving (10) to that in solving (9):

$$\gamma_{\text{OP}} := \frac{\|(Ay_* + x_{\text{init}}) - x_{\text{init}}\|}{\|x_* - x_{\text{init}}\|},$$

where we measure the optimization progress of a method by the Euclidean distance of its obtained solution to the initial one. The lower the value of γ_{OP} is, the more efficient solving (10) is compared to solving (9).

Table VIII reports results on the same tasks as in Section III. We utilize a subspace dimension of $\tilde{d} = 500$ (following BBT's default) and a reduced prompt length of $l = 5$ to fit the computational constraints of full-space CMA-ES (see Appendix III-C for detailed settings and a discussion on the fairness of this configuration). We find solving (9) always yields a lower training loss than solving (10), demonstrating superior prompts can be obtained by searching in the full space. Conversely, γ_{OP} is consistently close to 1 across all tasks. This implies that the subspace search does not effectively shorten the optimization trajectory. Instead, the projection primarily serves to circumvent the prohibitive computational costs of second-order methods in high dimensions, a challenge that can alternatively be addressed by employing simpler, scalable algorithms.

One may wonder if it is possible to trade the computation effort saved by solving (10) for a post-hoc improvement over

the obtained solution. We show that it is also unlikely. To verify this, consider the following metric, which we call relative post-hoc improvement (denoted by γ_{PI}), defined as

$$\gamma_{PI} = \frac{\|x_* - (Ay_* + x_{init})\|}{\|x_* - x_{init}\|}.$$

The numerator quantifies the additional effort required to close the gap between the solution obtained for (10) and that for (9). A value of γ_{PI} greater than 1 means improving post-hocly the solution of (10) could be even more expensive than directly solving (9). Unfortunately, as reported in the last column of Table VIII, we do find γ_{PI} is above 1 in all considered tasks. This indicates that the random subspace projection limits the achievable solution quality, creating a performance gap not effectively bridged by merely extending the search budget.

APPENDIX V MECHANISM OF CONFIDENCE REGULARIZATION

To understand the generalization gap in projection-free prompt search, we analyze the model behavior using two diagnostic metrics evaluated on the test set: **Prediction Probability** (\mathcal{P}) and **Global Rank** (\mathcal{R}).

Standard prediction strategies normalize probabilities only over the restricted verbalizer set \mathcal{W} , masking the model’s true uncertainty. To reveal this, we define Prediction Probability (\mathcal{P}) as the average probability assigned to the *predicted* verbalizer \hat{z} when normalized over the entire vocabulary \mathcal{V} . Formally:

$$\mathcal{P} = \frac{1}{|\mathcal{D}_{test}|} \sum_{(x) \in \mathcal{D}_{test}} \frac{\exp(\mathbf{h}_{\hat{z}})}{\sum_{v \in \mathcal{V}} \exp(\mathbf{h}_v)}, \quad (11)$$

where \hat{z} is the verbalizer with the highest logit within \mathcal{W} . A low \mathcal{P} implies that while the model selects \hat{z} from the candidates, it considers other irrelevant tokens in \mathcal{V} to be more probable. Complementarily, we employ Global Rank (\mathcal{R}), which computes the average rank of the *predicted* verbalizer’s logit within the full vocabulary \mathcal{V} . A rank closer to 1 indicates that the predicted label is naturally prioritized by the PLM without artificial constraints.

A. Analysis

We conducted a comparative analysis between SaES-ID (without regularization) and SaES-ID-CR (with regularization), with results summarized in Table IX.

A critical observation is that optimization without CR tends to exploit the restricted decision space. As evidenced by the extremely poor Global Rank (often exceeding hundreds) despite reasonable task metrics, standard SaES-ID finds prompts that marginally push the correct verbalizer above incorrect candidates within \mathcal{W} , while leaving them buried beneath unrelated functional tokens in the global distribution. These prompts effectively "game" the few-shot objective, achieving high training accuracy without establishing a robust semantic connection to the task. Such prompts are "correct for the wrong reasons" and are highly susceptible to overfitting the few-shot training examples.

In contrast, SaES-ID-CR aligns the prompt with the pre-training objective by enforcing high global probability. This constraint ensures that the prompt elicits the target concept as a natural language continuation, underpinning the superior generalization capability observed in the main results.

TABLE IX: Impact of Confidence Regularization on task performance and diagnostic metrics.

Task	Algorithm	Metric (%)	\mathcal{P}	\mathcal{R}
MRPC	SaES-ID	76.68 _{0.00}	0.0017	302.23
	SaES-ID-CR	81.26 _{0.11}	0.4710	16.80
MNLI	SaES-ID	46.40 _{1.64}	0.0099	221.48
	SaES-ID-CR	51.84 _{1.37}	0.0496	19.50
QQP	SaES-ID	49.51 _{3.21}	0.0017	203.45
	SaES-ID-CR	53.28 _{2.93}	0.3021	3.25
SST-2	SaES-ID	87.32 _{1.72}	0.0403	8.76
	SaES-ID-CR	90.25 _{0.47}	0.1655	1.58
RTE	SaES-ID	53.65 _{1.74}	0.0036	159.51
	SaES-ID-CR	57.47 _{1.83}	0.3188	5.32
CoLA	SaES-ID	3.86 _{2.18}	0.0007	342.53
	SaES-ID-CR	5.84 _{3.09}	0.3271	1.33
QNLI	SaES-ID	54.28 _{1.49}	0.0034	184.53
	SaES-ID-CR	60.10 _{2.20}	0.0036	128.52

REFERENCES

- [1] A. Vaswani, N. Shazeer, N. Parmar, J. Uszkoreit, L. Jones, A. N. Gomez, Ł. Kaiser, and I. Polosukhin, "Attention is all you need," *Advances in neural information processing systems*, vol. 30, 2017.
- [2] B. Min, H. Ross, E. Sulem, A. P. B. Veysch, T. H. Nguyen, O. Sainz, E. Agirre, I. Heintz, and D. Roth, "Recent advances in natural language processing via large pre-trained language models: A survey," *ACM Computing Surveys*, vol. 56, no. 2, pp. 1–40, 2023.
- [3] X. Qiu, T. Sun, Y. Xu, Y. Shao, N. Dai, and X. Huang, "Pre-trained models for natural language processing: A survey," *Science China technological sciences*, vol. 63, no. 10, pp. 1872–1897, 2020.
- [4] W. X. Zhao, K. Zhou, J. Li, T. Tang, X. Wang, Y. Hou, Y. Min, B. Zhang, J. Zhang, Z. Dong *et al.*, "A survey of large language models," *arXiv preprint arXiv:2303.18223*, vol. 1, no. 2, 2023.
- [5] J. Achiam, S. Adler, S. Agarwal, L. Ahmad, I. Akkaya, F. L. Aleman, D. Almeida, J. Altschmidt, S. Altman, S. Anadkat *et al.*, "GPT-4 technical report," *arXiv preprint arXiv:2303.08774*, 2023.
- [6] Y. Liu, M. Ott, N. Goyal, J. Du, M. Joshi, D. Chen, O. Levy, M. Lewis, L. Zettlemoyer, and V. Stoyanov, "RoBERTa: A robustly optimized BERT pretraining approach," *arXiv preprint arXiv:1907.11692*, 2019.
- [7] Y. Nesterov and V. Spokoiny, "Random gradient-free minimization of convex functions," *Foundations of Computational Mathematics*, vol. 17, no. 2, pp. 527–566, 2017.

- [8] J. Larson, M. Menickelly, and S. M. Wild, “Derivative-free optimization methods,” *Acta Numerica*, vol. 28, pp. 287–404, 2019.
- [9] T. Sun, Y. Shao, H. Qian, X. Huang, and X. Qiu, “Black-box tuning for language-model-as-a-service,” in *International Conference on Machine Learning*. PMLR, 2022, pp. 20 841–20 855.
- [10] N. Hansen, S. D. Müller, and P. Koumoutsakos, “Reducing the time complexity of the derandomized evolution strategy with covariance matrix adaptation (CMA-ES),” *Evolutionary computation*, vol. 11, no. 1, pp. 1–18, 2003.
- [11] T. Sun, Z. He, H. Qian, Y. Zhou, X. Huang, and X. Qiu, “BBTv2: Towards a gradient-free future with large language models,” *arXiv preprint arXiv:2205.11200*, 2022.
- [12] A. Aghajanyan, L. Zettlemoyer, and S. Gupta, “Intrinsic dimensionality explains the effectiveness of language model fine-tuning,” *arXiv preprint arXiv:2012.13255*, 2020.
- [13] E. Levina and P. Bickel, “Maximum likelihood estimation of intrinsic dimension,” *Advances in neural information processing systems*, vol. 17, 2004.
- [14] A. Wang, A. Singh, J. Michael, F. Hill, O. Levy, and S. R. Bowman, “GLUE: A multi-task benchmark and analysis platform for natural language understanding,” *arXiv preprint arXiv:1804.07461*, 2018.
- [15] Y. Akimoto, A. Auger, T. Glasmachers, and D. Morinaga, “Global linear convergence of evolution strategies on more than smooth strongly convex functions,” *SIAM Journal on Optimization*, vol. 32, no. 2, pp. 1402–1429, 2022.
- [16] S. Diao, Z. Huang, R. Xu, X. Li, Y. Lin, X. Zhou, and T. Zhang, “Black-box prompt learning for pre-trained language models,” *arXiv preprint arXiv:2201.08531*, 2022.
- [17] S. Zhang, S. Roller, N. Goyal, M. Artetxe, M. Chen, S. Chen, C. Dewan, M. Diab, X. Li, X. V. Lin *et al.*, “Opt: Open pre-trained transformer language models,” *arXiv preprint arXiv:2205.01068*, 2022.
- [18] E. Chávez, G. Navarro, R. Baeza-Yates, and J. L. Marroquín, “Searching in metric spaces,” *ACM computing surveys (CSUR)*, vol. 33, no. 3, pp. 273–321, 2001.
- [19] C. Li, H. Farkhor, R. Liu, and J. Yosinski, “Measuring the intrinsic dimension of objective landscapes,” *arXiv preprint arXiv:1804.08838*, 2018.
- [20] H. Zhang, H. Zhang, B. Gu, and Y. Chang, “Subspace selection based prompt tuning with nonconvex nonsmooth black-box optimization,” in *Proceedings of the 30th ACM SIGKDD Conference on Knowledge Discovery and Data Mining*, 2024, pp. 4179–4190.
- [21] H. Zhan, C. Chen, T. Ding, Z. Li, and R. Sun, “Unlocking black-box prompt tuning efficiency via zeroth-order optimization,” in *Findings of the Association for Computational Linguistics: EMNLP 2024*, 2024, pp. 14 825–14 838.
- [22] M. Deng, J. Wang, C.-P. Hsieh, Y. Wang, H. Guo, T. Shu, M. Song, E. P. Xing, and Z. Hu, “Rlprompt: Optimizing discrete text prompts with reinforcement learning,” *arXiv preprint arXiv:2205.12548*, 2022.
- [23] T. Brown, B. Mann, N. Ryder, M. Subbiah, J. D. Kaplan, P. Dhariwal, A. Neelakantan, P. Shyam, G. Sastry, A. Askell *et al.*, “Language models are few-shot learners,” *Advances in neural information processing systems*, vol. 33, pp. 1877–1901, 2020.
- [24] S. Ghadimi and G. Lan, “Stochastic first-and zeroth-order methods for nonconvex stochastic programming,” *SIAM journal on optimization*, vol. 23, no. 4, pp. 2341–2368, 2013.
- [25] B. Lester, R. Al-Rfou, and N. Constant, “The power of scale for parameter-efficient prompt tuning,” *arXiv preprint arXiv:2104.08691*, 2021.